Published OnlineFirst June 25, 2015; DOI: 10.1158/0008-5472.CAN-14-3510

Microenvironment and Immunology

Cancer Research

Nivolumab and Urelumab Enhance Antitumor Activity of Human T Lymphocytes Engrafted in Rag2$^{-/-}$IL2Rγ^{null} Immunodeficient Mice

Miguel F. Sanmamed[1,2], Inmaculada Rodriguez[2], Kurt A. Schalper[3], Carmen Oñate[2], Arantza Azpilikueta[2], Maria E. Rodriguez-Ruiz[1,2], Aizea Morales-Kastresana[2], Sara Labiano[2], Jose L. Pérez-Gracia[1], Salvador Martín-Algarra[1], Carlos Alfaro[2], Guillermo Mazzolini[4], Francesca Sarno[5], Manuel Hidalgo[5,6], Alan J. Korman[7], Maria Jure-Kunkel[8], and Ignacio Melero[1,2]

Abstract

A current pressing need in cancer immunology is the development of preclinical model systems that are immunocompetent for the study of human tumors. Here, we report the development of a humanized murine model that can be used to analyze the pharmacodynamics and antitumor properties of immunostimulatory monoclonal antibodies (mAb) in settings where the receptors targeted by the mAbs are expressed. Human lymphocytes transferred into immunodeficient mice underwent activation and redistribution to murine organs, where they exhibited cell-surface expression of hCD137 and hPD-1. Systemic lymphocyte infiltrations resulted in a lethal CD4$^+$ T cell–mediated disease (xenograft-versus-host disease), which was aggravated when murine subjects were administered clinical-grade anti-hCD137 (urelumab) and anti-hPD-1 (nivolumab). In mice engrafted with human colorectal HT-29 carcinoma cells and allogeneic human peripheral blood mononuclear cells (PBMC), or with a patient-derived gastric carcinoma and PBMCs from the same patient, we found that coadministration of urelumab and nivolumab was sufficient to significantly slow tumor growth. Correlated with this result were increased numbers of activated human T lymphocytes producing IFNγ and decreased numbers of human regulatory T lymphocytes in the tumor xenografts, possibly explaining the efficacy of the therapeutic regimen. Our results offer a proof of concept for the use of humanized mouse models for surrogate efficacy and histology investigations of immune checkpoint drugs and their combinations. *Cancer Res; 75(17); 3466–78. ©2015 AACR.*

Introduction

Cancer immunotherapy has been boosted in the clinic with the advent of immunostimulatory monoclonal antibodies (mAb; refs. 1, 2). The concept behind this ongoing revolution is that the function of cells of the immune system can be modulated by antibody molecules binding to receptors expressed on their cell surface.

Mouse models in the late 1990s showed that this goal could be attained by antagonist antibodies directed against CTLA-4 (CD152; ref. 3) and agonist antibodies directed at CD137 (4-1BB, TNFRSF9; ref. 4), with complete rejections of transplanted tumors being achieved. The list of antibody specificities exerting this type of effect in mice has grown and now encompasses antagonists of PD-1, PD-L1/B7-H1, TIM-3, LAG-3, and agonists of OX-40, GITR, CD40, and CD27 (5–7).

Antagonist mAbs anti-CTLA-4 have been developed in the clinic (8, 9). One of these (ipilimumab) has shown evidence of clinical benefit (9, 10) in patients with metastatic melanoma at the expense of a new type of adverse effects evoking organ-specific autoimmune reactions (11). More recently, mAbs blocking PD-1 to PD-L1/B7-H1 interactions have been tested in melanoma, renal cell carcinoma, bladder carcinoma, Hodgkin lymphoma, and non–small cell lung cancer patients (12–17). The exciting picture that emerges from phase I clinical trials and their cohort extensions is that an important fraction of patients shows durable objective clinical responses (18). The previous success has prompted a number ongoing registration phase III clinical trials. Available information indicates a clear tendency for increased benefit in patients whose tumor cells express surface PD-L1/B7-H1, although responses are also evoked in a fraction of PD-L1–negative cases (19). A pioneering trial using combinations of ipilimumab with nivolumab (anti-hPD-1 mAb) has shown very rapid and profound objective clinical responses (≥80% decline in tumor burden at week 12) in metastatic melanoma patients with 53% response rates at the maximum-tolerated dose (20). These results recently confirmed in a randomized phase II clinical trial (21) have been conducive

[1]Department of Oncology, Clínica Universidad de Navarra, Pamplona, Spain. [2]Centro de investigación médica aplicada (CIMA), Universidad de Navarra, Pamplona, Spain. [3]Department of Pathology, Yale School of Medicine, New Haven, Connecticut. [4]Gene Therapy Laboratory, Department of Medicine, Universidad Austral, Pilar, Argentina. [5]Centro Integral Oncológico Clara Campal (CIOCC), Madrid, Spain. [6]Spanish National Cancer Research Centre (CNIO), Madrid, Spain. [7]Biologics Discovery California, Bristol-Myers Squibb, Redwood City, California. [8]Bristol-Myers Squibb Company, Princeton, New Jersey.

Note: Supplementary data for this article are available at Cancer Research Online (http://cancerres.aacrjournals.org/).

Corresponding Author: Ignacio Melero, Centro de investigación médica aplicada (CIMA) Avenida PIO XII, 55 31008 Pamplona, Spain. Phone: 34-948-194700; Fax: 34-948-194700; E-mail: imelero@unav.es

doi: 10.1158/0008-5472.CAN-14-3510

Published OnlineFirst June 25, 2015; DOI: 10.1158/0008-5472.CAN-14-3510

to an ongoing phase III clinical trial of this combinatorial immunotherapy (NCT01844505).

Two anti-CD137 mAb are currently undergoing clinical development: urelumab and PF-05082566. Urelumab has been tested at doses ranging from 0.1 to 10 mg/kg. At high doses, a fraction of patients developed hepatitis that was severe in some cases, including two fatalities (22). The safety of lower doses is currently being retested (NCT00309023). Interest in these antibodies has increased because it has been discovered that, in addition to boosting antitumor CD8 T-cell responses, anti-CD137 mAb enhance antibody-dependent cellular cytotoxicity, thereby synergizing with rituximab (23), trastuzumab (24), and cetuximab (25) in preclinical models. Clinical trials testing combinations of anti-hCD137 mAbs with rituximab and cetuximab are also ongoing (NCT01307267, NCT01775631). The combination of nivolumab and urelumab has recently started phase I dose-escalation clinical trials (NCT02253992) also undertaken with a combination of the anti-PD-1 mAb pembrolizumab and PF-05082566 (NCT02179918).

Suitable and predictive animal models to study the effect of immunotherapy are an unmet need. Ideally, models would allow different immunostimulatory mAbs to be combined and the cellular and molecular events governing efficacy and adverse events to be characterized. In these animal experiments, the best sequence of immunotherapy agents could be chosen, the mechanism of action understood, and potential predictive biomarkers defined. Human T lymphocytes, including peripheral blood lymphocytes, from cancer patients can be grafted into immunodeficient mice strains. There are two main mouse strains that are commonly used: nonobese diabetic (NOD)-severe combined immunodeficient (*scid*) and recombinant activating one or two gene deficient ($Rag1^{-/-}$ and $Rag2^{-/-}$). These strains can be crossed to interleukin-2 receptor common γ chain targeted mutation ($IL2r\gamma^{null}$) mice, which completely ablates natural killer (NK) cell activity and enhances human cells engraftment. Engrafted human T lymphocytes show xeno-reactivity against foreign major histocompatibility (MHC) class I and II and other antigens from the mice cells (26). As a result, T lymphocytes cause an inflammatory infiltrate in different organs that leads to wasting and death of the animals after several weeks, a process known as xenograft-versus-host disease (xGVHD; ref. 27). The transferred human T lymphocytes are amenable to regulation by therapeutic agents or adoptively transferred other immune cells such regulatory T cells (Treg). In this regard, xGVHD has been exploited to study the molecular mechanisms of immunosuppression and immunomodulatory therapies (28–31).

We have confirmed the activation of human peripheral blood lymphocytes after being xenografted in immunodeficient $Rag2^{-/-}IL2R\gamma^{null}$ mice. As a result of becoming activated, transferred human T lymphocytes express the inducible surface antigens hPD-1 and hCD137 on their plasma membrane. This allowed tests on the *in vivo* activity of the immunotherapeutic mAbs urelumab (anti-hCD137) and nivolumab (anti-hPD-1), both in the context of the xGVHD and immunity against concurrently xenografted human tumors.

Materials and Methods

Mice

$Rag2^{-/-}IL2R\gamma^{null}$ mice were purchased from The Jackson Laboratory and C57/BL6 wild-type mice were purchased from Harlan Laboratories and bred at Centro de investigación médica aplicada (CIMA; Pamplona, Spain) under specific pathogen-free conditions. Animal experiments were in accordance with Spanish laws and approval was obtained from the animal experimentation committee of the University of Navarra (Pamplona, Spain; reference 172-12 approval).

Cell lines and primary tumor explants

The human colon cancer–derived HT-29 cell line (ATCC HTB-38) was purchased from the American Type Culture Collection in 2013. A master cell bank was expanded upon arrival and a new ampule is thawed every 4 months for experimentation. Cells were cultured in RPMI-1640 supplemented with 10% heat-inactivated fetal bovine serum and 1% penicillin–streptomycin, all from Life Technologies. The murine colon adenocarcinoma cell MC38 is a colon adenocarcinoma cell line of C57BL/6 origin whose identity has been verified by Idexx Radil (Case 6592-2012) and kept in the master cell bank. This cell line was originally provided to us by Dr. Karl E. Hellström (Harborview Medical Center, University of Washington, Seattle, WA) and cultured in RPMI-1640-GlutaMax medium supplemented with 10% fetal bovine serum (Gibco) and 50 mol/L 2-mercaptoethanol. A second-pass human gastric carcinoma explant obtained from a surgical specimen of a gastric cancer donor patient, was generated at HM Universitario Sanchinarro (CIOCC; Madrid, Spain; protocol approval FHM.06.10), as described previously (32).

Antibodies and human peripheral blood mononuclear cells

The following antibodies were developed, produced, and quality controlled at Bristol-Myers Squibb facilities: nivolumab (a fully human IgG4 anti-human PD-1); urelumab (a fully human IgG4 anti-human CD137); and irrelevant human IgG4 as an isotype-matched control. Therapeutic anti-CD137 (clone 1D8), anti-PD-1 (clone RMP1-14), anti-CD4 (clone GK1.5), anti-CD8 (clone 2.43), and anti-NK1.1 (clone PK136) mAbs were produced and purified by affinity chromatography on protein-G from the corresponding hybridomas. Peripheral blood mononuclear cells (PBMC) were isolated from buffy coats provided by the blood bank of Navarra, Spain, after written informed consent (Ethics Committee from the University Clinic of Navarra 007/2007 and 013/2009) or from 30 mL peripheral blood samples drawn from the gastric carcinoma patient, on three occasions, under individual informed consent (protocol approval FHM.06.10).

Collection of transferred lymphocytes in mice peritoneum

$Rag2^{-/-}IL2R\gamma^{null}$ mice were injected with 1×10^7 human PBMCs intraperitoneally (i.p.). Peritoneal lavages were performed at different time points and the recovered cells were analyzed by flow cytometry.

xGVHD model

Three- to 4-week-old $Rag2^{-/-}IL2R\gamma^{null}$ mice were injected with 1×10^7 human fresh PBMCs i.p. on day 0 of the experiment. Treatment with anti-hCD137 (urelumab, 200 μg per injection), anti-hPD-1 (nivolumab, 200 μg per injection), Combo (nivolumab + urelumab, 200 μg per injection each), or saline control was administered by intravenous (i.v.) injection on days 4, 7, and 10. Plasma samples were prepared from blood collected in heparin tubes 1 day before the first injection of treatment and after the first and second injection of the mAbs. Plasma samples were stored at −80°C until use. Survival and xenograft-versus-host reaction was

Published OnlineFirst June 25, 2015; DOI: 10.1158/0008-5472.CAN-14-3510

monitored daily up to 3 months. Animals that developed clinical symptoms of xGVHD (>15% weight loss, hunched posture, reduced mobility, fur loss, tachypnea) were sacrificed and an endpoint of survival was recorded. In some experiments mice were sacrificed on day 22 and lung and liver were surgically removed, weighed, and processed for immunohistochemistry (IHC) and flow cytometry analysis.

Tumor experiments

Three- to 4-week Rag2$^{-/-}$IL2Rγ^{null} mice old were injected with 7×10^6 human fresh PBMCs i.p. and a total of 3.5×10^6 HT29 human colon carcinoma cells were injected subcutaneously (s.c.) into the flank of Rag2$^{-/-}$IL2Rγ^{null} mice in 50 μL of PBS on day 0 of the experiment. Mice were treated intravenously with anti-hCD137 (urelumab, 200 μg per injection), anti-hPD-1 (nivolumab, 200 μg per injection), Combo (nivolumab + urelumab, 200 μg per injection each), or isotype-matched control (200 μg of irrelevant hIgG4) on days 6, 14, and 20. Plasma samples were prepared from blood collected in heparin 1 day before the first injection of treatment and after the first and second injection. Plasma samples were stored at −80°C until use. Tumor growth was recorded every 3 to 4 days. Mice were sacrificed on day 22 and s.c. tumors were removed, weighed, and processed for IHC and flow cytometry analysis.

In addition, 3- to 4-week-old Rag2$^{-/-}$IL2Rγ^{null} mice were injected i.p. with 2 or 7×10^6 human PBMCs from a gastric cancer patient on day 0 of experiment. Explants (7 mm × 7 mm) from the tumor of the same patient were implanted s.c. into the flank of Rag2$^{-/-}$ IL2Rγ^{null} mice on day 3 of the experiment. Mice were treated i.v. as indicated above on days 5, 12, and 19. Tumor growth was monitored every 3 to 4 days. On day 22 of experiment mice were sacrificed, tumors removed, and studied by quantitative immunofluorescence (QIF). Tumor growth analyses were limited to 3 to 4 weeks because following this period of time mice started to show signs of xGVHD.

Immunohistochemistry

Tissues were recovered from mice at necropsy, formalin-fixed and embedded in paraffin. IHC was performed using the following mAbs against CD3 (clone SP7), CD4 (clone SP35), and CD8 (clone SP6). Details are provided in the Supplementary Methods Appendix.

Multiplexed quantitative immunofluorescence

QIF was performed using multiplexing panels including antibodies against human cytokeratin (hCK, clone AE1/AE3) and mAbs against hCD137 (clone GW2.4), hPD-1 (clone 5C3), and hPD-L1 (clone E1L3N; ref. 33). Additional QIF studies included simultaneous detection of hCK (clone M3515), hCD3 (clone E272), hCD8 (clone C8/144B), and hCD20 (clone L26) as recently described (34). Details are provided in the Supplementary Methods Appendix.

Antibodies and flow cytometry

Lung, liver, and tumor tissue was processed for flow cytometry analysis. Fluorochrome-conjugated mAbs to the following human antigens were used: CD3 (UCHT1), CD4 (OKT4), CD8 (RPAT8), CD45 (HI30), FoxP3 (150D), Ki-67 (B56), CD279/PD-1 (EH12.2H7), TIM-3 (F38-2E2), and PD-L1/B7-H1 (29E.2A3) from BioLegend; CD25 (BC96), Eomes (WD1928), and LAG-3 (3DS223H) from eBioscience, CD137 (5D1; ref. 35) and Perforin (deltaG9) from BD Pharmigen. FACSCanto II and FACSCalibur (BD Biosciences) were used for cell acquisition and data analysis was carried out using the FlowJo software (TreeStar Inc.). Details are provided in the Supplementary Methods Appendix.

ELISA assays

Levels of human IFNγ and human TNFα in mouse plasma samples were measured by a commercial enzyme linked immunosorbent assay (ELISA; Human IFNγ Elisa Set, BD OptEIA, BD Biosciences and Human TNFα Elisa Development Kit; Peprotech), according to the manufacturer's instructions. All samples were measured in duplicate. The detection cutoff levels of the assay were 4.7 and 15 pg/mL for IFNγ and TNFα, respectively. The coefficient of variation was <15%.

Statistical analysis

Statistical analyses were performed with the Prism 6.0 software (GraphPad Software) Macintosh version. The nonparametric Mann–Whitney *U* test was applied to compare the results between groups of treatment. Survival curves were analyzed by the Kaplan–Meier method and compared by log-rank tests. Growth of tumors was compared by a nonlinear regression analysis. A two-tailed $P \leq 0.05$ was considered as statistically significant.

Results

Activation and expression of the targets for immunostimulatory mAbs on human T lymphocytes engrafted in immunodeficient mice

Rag2$^{-/-}$IL2Rγ^{null} mice are devoid of T, B, and NK lymphocytes. Intraperitoneal injection of human PBMC gives rise to the engraftment of viable CD4$^+$ and CD8$^+$ T lymphocytes that can be sequentially retrieved by peritoneal lavage over 4 weeks following adoptive transfer. It is well known that human T lymphocytes develop pathogenic xeno-reactivity when they are transferred into mice and become activated (27). hCD3$^+$-gated T cells such as hCD4$^+$ and hCD8$^+$ T lymphocytes underwent blastic activation, which peaked on days 5 to 9 (Fig. 1A and Supplementary Fig. S1A), as shown by enlargement revealed by the forward scatter and side scatter parameters. Such T lymphocytes underwent proliferation as observed by intracellular immunostaining with Ki-67 on gated hCD4$^+$ and hCD8$^+$ T cells from the sequential peritoneal lavages (Fig. 1B and Supplementary Fig. S1B). The activation/exhaustion markers TIM-3 and LAG-3 have also been studied showing an initial activation during first 5 days and a second peak of coexpression with PD-1 that might reflect T lymphocyte exhaustion after 4 weeks (Supplementary Fig. S1C).

CD137 and PD-1 are respectively important receptors for costimulation and coinhibition of T cells whose expression on the plasma membrane is known to be induced by antigen stimulation. Figure 1C shows that both receptors were induced on the adoptively transferred human lymphocytes over time. hCD137 was induced mainly on hCD8$^+$ T lymphocytes, while hPD-1 was induced on both T-cell subsets with very bright intensity. PD-1 ligand 1 (PD-L1/B7-H1) was also induced in T cells, with a peak on day 5 (Supplementary Fig. S1D).

To analyze whether anti-hCD137 (urelumab) and anti-hPD-1 (nivolumab) mAbs were binding to their corresponding receptors *in vivo*, flow cytometry of transferred lymphocytes was performed *ex vivo*. As shown in Supplementary Fig. S2, the fluorescence intensity of CD137 and PD-1 staining was decreased on human

Published OnlineFirst June 25, 2015; DOI: 10.1158/0008-5472.CAN-14-3510

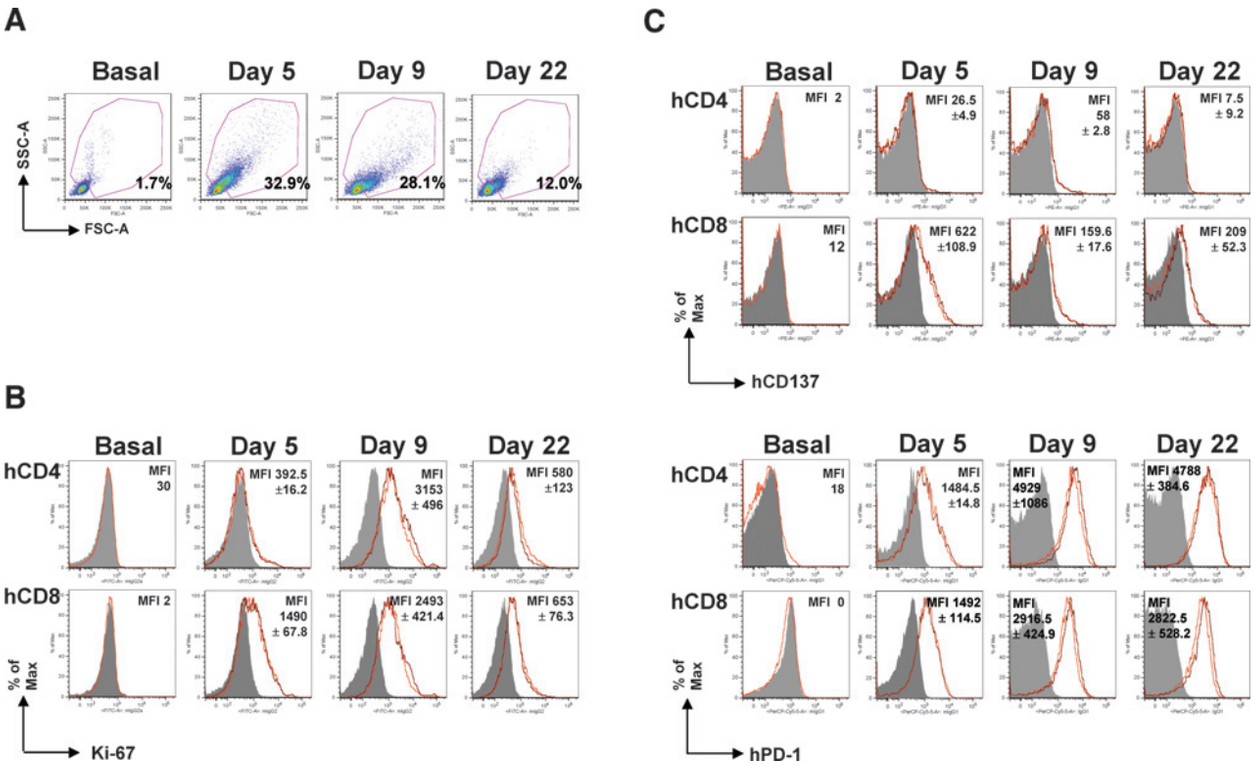

Figure 1.
Human T cells acquire an activated phenotype and express surface CD137 and PD-1 after being transferred into Rag2$^{-/-}$IL2Rγ^{null} mice. Rag2$^{-/-}$IL2Rγ^{null} mice were injected with 1×10^7 human PBMCs i.p. on day 0. Peritoneal lavages were performed in two mice/day at days 1, 3, 5, 7, 9, 13, 22, and 30 and the cells recovered were analyzed by flow cytometry. A, percentage of hCD3$^+$ blasts lymphocytes recovered from the peritoneal lavage at the indicated time points. B and C, level of Ki-67 intranuclear staining (B) and hCD137 (top) and hPD-1 (bottom) surface staining represented by mean fluorescence intensity (MFI) on gated hCD3$^+$hCD4$^+$ and hCD3$^+$hCD8$^+$ T cells before transfer and on day 5, 9, and 22 after adoptive transfer (C). Shadowed histograms respresent isotype-matched control stainings.

T cells recovered from anti-hCD137 and anti-hPD-1–treated mice, but not on T cells from untreated mice.

These data confirm that transferred human T lymphocytes in Rag2$^{-/-}$IL2Rγ^{null} become activated during the first 7 days and consequently express on the cell-surface hCD137 and hPD-1, thus becoming susceptible targets to be manipulated by immunomodulatory mAbs.

Adoptive transfer of human T lymphocytes causes a xenograft versus host disease that is exacerbated by urelumab and nivolumab and abrogated by CD4$^+$ depletion

xGVHD is considered a valuable model to test immunomodulatory strategies, where the engrafted human T lymphocytes are amenable for regulation by therapeutic agents (29, 31). After 3 to 4 weeks we observed that transferred T lymphocytes started to infiltrate the spleen, liver, and lung with signs of serious tissue damage after 4 to 5 weeks (Supplementary Fig. S3). Accordingly, we observed that mice injected with 10^7 human PBMC (Fig. 2A) started losing weight at 3 to 4 weeks after adoptive transfer and in most instances succumbed 1 week later showing signs of respiratory distress, hunched posture, and/or fur loss.

Having confirmed the expression of hCD137 and hPD-1 in human T lymphocytes infiltrating the liver and spleen (Supplementary Fig. S4), we tested whether the administration of immunostimulatory mAbs exacerbated xGVHD. We injected mice with 10^7 human PBMC and treated them with the clinical-grade mAbs urelumab (anti-hCD137), nivolumab (anti-hPD-1), a combination of the two (Combo) or saline (control) on days 4, 7, and 10 after lymphocyte transfer. Mice were followed for lethal xGVHD and a significant decrease in overall survival was observed in the nivolumab ($P < 0.001$) and Combo ($P < 0.05$) groups as compared with the control group, while urelumab showed a tendency that did not reach statistical significance (Fig. 2B). Details of the H&E and CD3$^+$ spleen, liver, and lung infiltration in a representative mouse of each group of treatment are depicted in Fig. 2C, showing marked perivascular T lymphocyte infiltrations in these organs, more intense when under treatment with the mAbs. To understand the role of specific immune cell subsets, we repeated the xGVHD model injecting hPBMC that were selectively predepleted of specific leukocyte subpopulations by immunomagnetic sorting. These included selective depletions of CD4$^+$, Treg, CD8$^+$, CD56$^+$, and CD14$^+$ populations checked to be complete by flow cytometry (data not shown). Transferred mice were treated with Combo (nivolumab and urelumab mAbs). The control group was injected with hPBMC and treated with hIgG4. Notably, mice injected with hPBMC depleted from CD4$^+$T cells did not develop xGVHD and survival, extended over 80 days, was significantly higher than mice injected with hPBMC and treated with Combo ($P < 0.01$) or hIgG4 ($P < 0.01$; Supplementary Fig. S5A). Depletion of other immune cells did not significantly affect the survival of

Published OnlineFirst June 25, 2015; DOI: 10.1158/0008-5472.CAN-14-3510

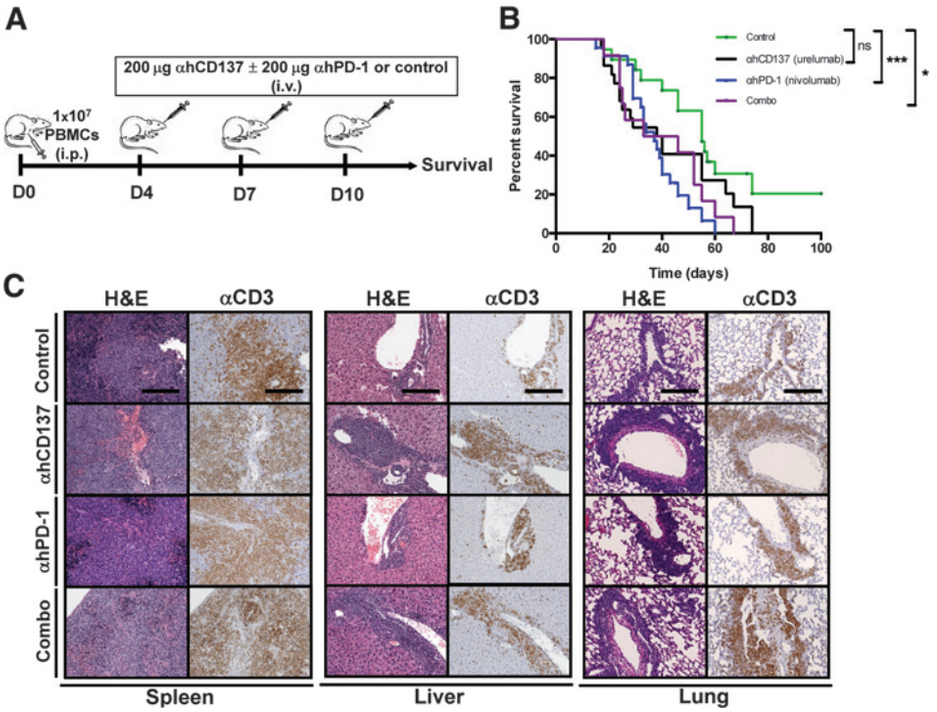

Figure 2.
Administration of anti-hPD-1 mAb (nivolumab) as a single agent or in combination with anti-hCD137 (urelumab) exacerbates xGVHD mediated by human PBMCs in Rag2$^{-/-}$IL2Rγ^{null} mice. A, Rag2$^{-/-}$IL2Rγ^{null} mice were injected with 10^7 human PBMCs i.p. on day 0. Treatments with anti-hCD137 (urelumab), anti-hPD-1 (nivolumab), combination (Combo; urelumab+nivolumab), or saline control i.v. were injected on days 4, 7, and 10. Survival was monitored up to 100 days. B, the Kaplan–Meier plot depicts overall survival among the four groups of treatment urelumab ($n = 22$), nivolumab ($n = 23$), combination (Combo; $n = 13$), and control ($n = 19$). Experiments were independently repeated three times and results pooled. *, $P < 0.5$; ***, $P < 0.001$. C, microphotographs of H&E and hCD3 IHC stainings in representative tissue sections of spleen, liver, and lung in one representative mouse from each group of treatment. Bar, 400 μm.

mice and only Treg depletion showed a trend to increase the severity of xGVHD, in comparison with mice injected with hPBMC and treated with Combo (Supplementary Fig. S5B). Notably, human-IFNγ plasma levels were almost undetectable in mice transferred without CD4$^+$ T cells (Supplementary Fig. S5C).

As a whole, these data indicate that the administration of the mAbs was active, resulting in enhanced functional stimulation of transferred T cells that migrate to visceral organs and exacerbate a xGVHD that is primarily driven by IFNγ-producing CD4$^+$ T lymphocytes.

Urelumab and nivolumab enhance the functional activation of adoptively transferred human T lymphocytes

A hallmark function of activated T lymphocytes is the production of cytokines. Therefore, we studied the concentrations of human IFNγ (hIFNγ) in sequential plasma samples of mice undergoing treatment with urelumab, nivolumab, the combination (Combo) or the control group. Following the second dose, urelumab-treated mice showed an increase of hIFNγ plasma levels in comparison with the control group ($P < 0.05$; Fig. 3A). Nivolumab as a single agent did not significantly increase hIFNγ plasma levels, but in combination with urelumab there was a further increase of plasma over control or nivolumab single treatment ($P < 0.01$). Production of this cytokine might depend on lymphocyte numbers producing it. Indeed, we observed that mice treated with urelumab or Combo, showed higher densities of blastic hCD3$^+$ and hCD8$^+$ lymphocytes in the liver infiltrates (Fig. 3B).

It is also possible that antibody treatment may result in functional changes on a per-cell basis. In this regard, we observed that in animals treated with nivolumab lung-infiltrating hCD4$^+$ and hCD8$^+$ T lymphocytes showed higher intensity of expression of the intracellular cytotoxic effector molecule perforin in comparison with control group (Fig. 3C).

Xenografted human colorectal carcinoma is controlled by allogeneic human PBMC under stimulation with urelumab and/or nivolumab

The experimental setting described in Rag2$^{-/-}$IL2Rγ^{null} mice permits both transfer of human PBMC and the grafting of subcutaneous tumors derived from transplantable human cell lines. We used the HT29 human colorectal carcinoma cell line that gives rise to rapidly progressing subcutaneous tumors in these mice (36). To explore if under these conditions anti-hCD137, anti-hPD-1, or their combination could interfere with tumor progression, we treated these mice with urelumab, nivolumab, Combo (urelumab+nivolumab), or isotype control (irrelevant hIgG4) on days 6, 14, and 20 as depicted in Fig. 4A.

We individually followed tumor growth over time. In a series of three experiments, it became clear that control mice without hPBMC experienced a faster tumor growth than those mice with concomitant adoptive transferred of hPBMC. Under these conditions, treatment with the immunostimulatory mAbs led to a clear stabilization of the experimental tumors in most instances that was of comparable efficacy to each antibody administered separately or in combination ($P < 0.001$; Fig. 4B). Indeed, the plasma of the mice under treatment showed significantly higher concentrations of hIFNγ after the second antibody dose as compared with the control group ($P < 0.05$; Fig. 4C). After the first dose a significant increase ($P < 0.05$) in TNFα plasma levels was also observed in the Combo-treated group in contrast with the control (irrelevant hIgG4) group (data not shown).

As a control, mice bearing HT29 human tumors but without hPBMC transfer did not show any improvement upon Combo

Published OnlineFirst June 25, 2015; DOI: 10.1158/0008-5472.CAN-14-3510

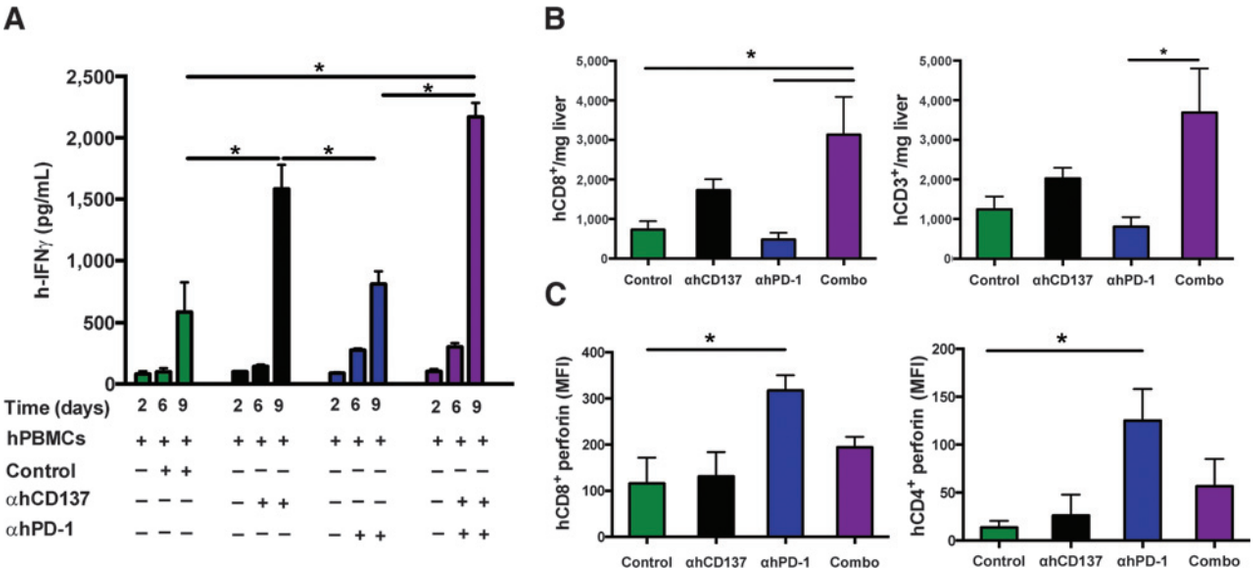

Figure 3.
Evidence for enhanced xenoreactive human lymphocyte activity upon treatment with anti-hCD137 (urelumab), anti-hPD-1 (nivolumab), and their combination. Experiments performed as in Fig. 2A. A, human IFNγ plasma levels of mice were studied before the first mAb dose and after the first (day 6) and second (day 9) doses of antibodies. B and C, mice were sacrificed at week 3 after human PBMCs transfer and single-cell suspensions were prepared from the lung, liver, spleen, and peritoneal lavage to be studied by flow cytometry. B, absolute numbers of $hCD3^+$ (right) and $hCD8^+$ (left) per gram of tissue in the liver. C, perforin mean fluorescence intensity (MFI) of $hCD3^+hCD8^+$ (left) and $hCD3^+hCD4^+$ (right) in the lung lymphocyte infiltrates. Data were analyzed by the Mann–Whitney *U* test. *, $P < 0.05$; **, $P < 0.01$. Error bars represent SEM.

treatment when compared with the hIgG4-treated control group (Supplementary Fig. S6).

To evaluate the role of the different immune cells controlling tumor growth, we tested the combination of anti-mCD137 (clone 1D8) and anti-mPD1 (clone RMP1-14) mAbs in a murine syngeneic model bearing murine colon cancer (MC38). We found that depletion of $CD8^+$ cells significantly abrogate the antitumor effect of the combinatorial treatment, while CD4, NK, or macrophage depletions did not affect the antitumor effect with the combinatorial treatment (Supplementary Fig. S7).

Studying cell suspensions of tumor-infiltrating lymphocytes

To address the mechanism of action of urelumab and nivolumab either alone or in combination, the human $CD4^+$ and $CD8^+$ T lymphocyte density was analyzed in tumors excised on day 22 from the experimental groups of mice, as depicted in Fig. 4A. The Combo treatment led to more dense infiltrates of $hCD8^+$ T lymphocytes in comparison with control group ($P < 0.001$) and also in comparison with each antibody given alone (urelumab, $P < 0.01$; nivolumab, $P < 0.05$; Fig. 4D, left).

The role of regulatory T lymphocytes is known to be important in dampening antitumor immunity (37). We observed that treatment with urelumab alone or in combination with nivolumab showed a significant improvement in the intratumoral $hCD8^+$ T cells/$hCD4^+FOXP3^+$ ratio when compared with the control group ($P < 0.01$; Fig. 4D, right). In the group in which urelumab was administered as a single agent, it seems that this improvement is dependent of a significant decrease in Treg number per gram of tumor tissue (Fig. 4D, center), while in the Combo group it is more dependent on an increase in total CD8 T cells over Tregs (Fig. 4D, left). Of note, tumor-infiltrating lymphocytes (TIL) under treatment with urelumab or Combo showed a tendency to express higher protein levels of the transcription factor EOMES in $hCD4^+$ and $hCD8^+$ T cells on a per cell basis, when analyzed by intracellular staining (data not shown).

Pathologic examination of tumors excised on day 22 (Fig. 5) showed denser infiltrates of human T cells upon treatment with the immunostimulatory mAbs that progressed inwards from the peripheral rim of the tumors and sparsely reached to the core of the round tumor lesions. Indeed, both the densities of human $hCD4^+$ and $hCD8^+$ T cells were increased. In the case of mice treated by the Combo treatment, the infiltrate was denser than in the single-agent treatment tissue samples, and human T cells infiltrated more clearly the central part of the tumor lesions (Fig. 5).

PD-L1/B7-h1, hPD-1, and hCD137 are present in the xenografted tumors

PD-L1/B7-H1 is known to be induced on malignant cells by inflammatory lymphokines such as IFNγ. Hence, it is considered an adaptive mechanism of resistance to immune attack (38). Indeed, HT-29 cells cultured in the presence of hIFNγ readily upregulate surface PD-L1/B7-H1 (data not shown). Analyzing the xenografted tumors under treatment using multiplexed immunofluorescence, which highlight the mAb targets as well as the tumor cells, it became clear that carcinoma cells were indeed expressing PD-L1/B7-H1 (Fig. 6 and Supplementary Fig. S8). PD-1 signal was allocated predominantly in lymphoid cells at the periphery of the neoplasms and PD-L1 staining was higher toward the tumor center/core. Both markers showed predominant membranous staining pattern (Supplementary Fig. S8). The proportion of cytokeratin-positive tumor cells was prominently lower and the PD-L1 signal, in these cells, was higher in the Combo treatment than in the control condition (Fig. 6 and Supplementary Fig. S9).

Published OnlineFirst June 25, 2015; DOI: 10.1158/0008-5472.CAN-14-3510

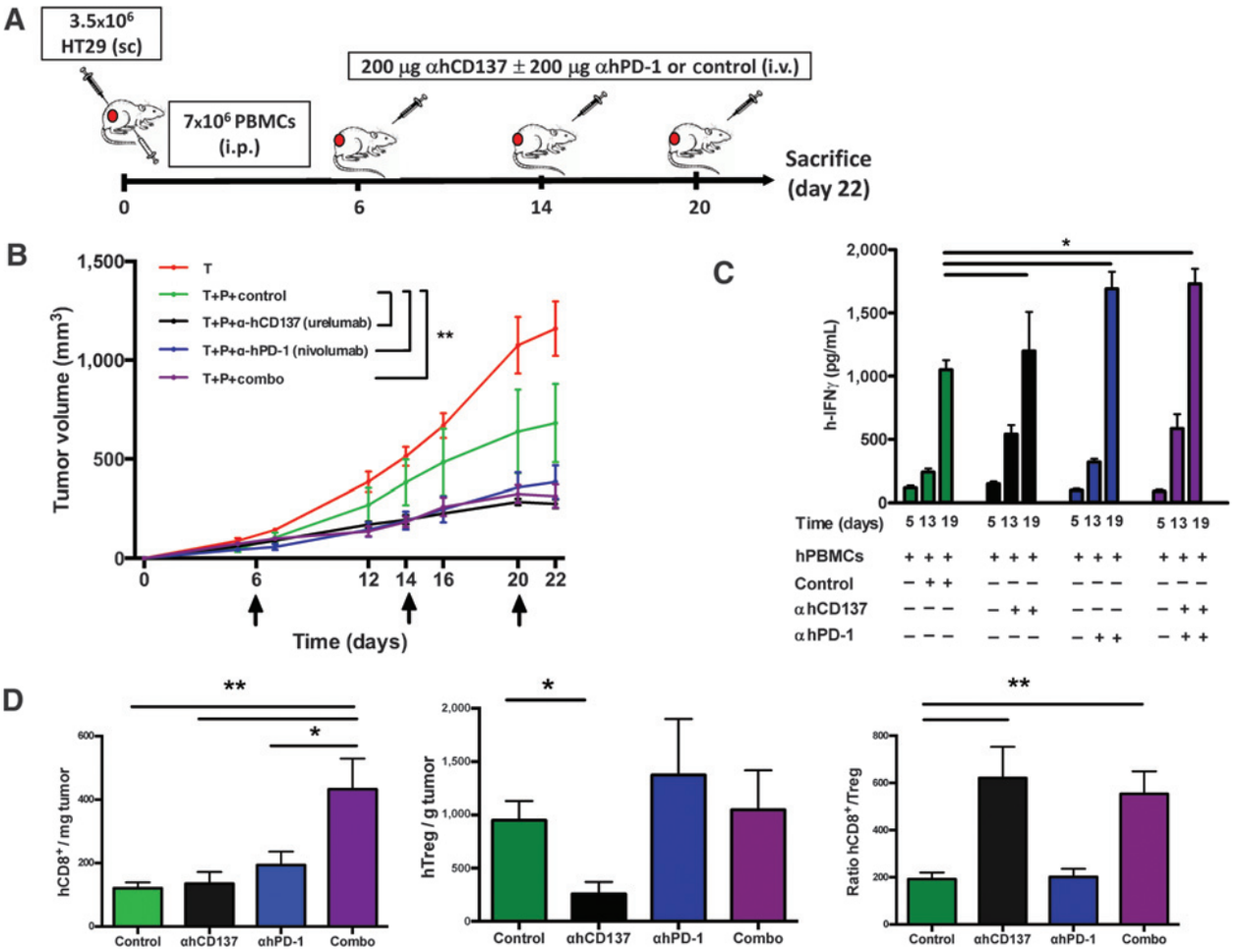

Figure 4.
Immunostimulatory mAbs anti-hCD137 (urelumab) and anti-hPD-1 (nivolumab) alone or in combination show antitumor activity against a xenografted human colon cancer mediated by transferred allogeneic human PBMC. A, $Rag2^{-/-}IL2R\gamma^{null}$ mice were injected with 7×10^6 human PBMCs i.p. and challenged with 3.5×10^6 HT-29 cells s.c. in the right flank on day 0 of the experiment. Thereafter, the mice were treated with anti-hCD137 (urelumab), anti-hPD-1 (nivolumab), combination (urelumab+nivolumab), or isotype control (hIgG4) i.v. on days 6, 14, and 20. Tumor volumes were measured twice per week until mice were sacrificed on day 22 of experiment. Tumors were removed after sacrifice and studied by flow cytometry and IHC. B, results depict mean ± SEM of the progression of subcutaneous tumor volumes ($n = 5$ mice per group). Arrows, time of treatment administration. Experiments were repeated four times, rendering similar results. C, human IFNγ plasma levels were studied previous to the first mAb dose, after the first and second antibody dose. D, tumor TILs from each treatment group were studied by flow cytometry and results of number of human CD8 T lymphocytes per mg of tumor (left), number of human regulator T cells per gram of tumor (center graph), and ratio of number of human CD8 T cells per number of human Treg (right) are depicted. *, $P < 0.05$; **, $P < 0.01$. Error bars represent SEM. T, tumor; P, hPBMCs.

It is of note that the TILs in those tumors under treatment showed as well membrane expression of hCD137 (Fig. 6). Taken together, these results demonstrate that the hPD-1–PD-L1 pathway and hCD137 are available targets in the tumor infiltrate to be modulated by the exogenously provided mAbs. In addition, the selective expression of PD-L1/B7-H1 toward the center of the tumor, right beneath a peripheral rim enriched in $hCD3^+/hCD137^+/hPD\text{-}1^+$, suggests that these T lymphocytes are in an activated state but may not be able to gain access to the PD-L1 enriched tumor core. Thus, such T cells are conceivably amenable to be both unrepressed and costimulated to further increase tumor cell destruction.

Therapeutic control of a xenografted gastric cancer by syngenic PBMC upon treatment with urelumab and nivolumab

To explore these mechanisms in a tumor-lymphocyte autologous setting, we xenografted tumor pieces (7 mm × 7 mm) derived from a surgical specimen of a gastric carcinoma patient in $Rag2^{-/-}IL2R\gamma^{null}$ mice and preinfused these mice with 7×10^6 PBMC from the same patient. Mice were treated intravenously with urelumab, nivolumab, Combo (urelumab+nivolumab), or isotype control (hIgG4) on days 5, 12, and 19 of the experiment. As shown in Fig. 7A, repeated antibody treatment resulted in a significantly slower progression in tumor size in all the treatment groups in contrast with the control group (urelumab $P < 0.001$; nivolumab $P < 0.05$; Combo $P < 0.01$). Analysis of hIFNγ levels in plasma showed a progressive increase during treatment with a tendency to increased levels in the urelumab monotherapy and Combo groups in contrast with control group and nivolumab monotherapy (Fig. 7B). We confirmed the same result in a second experiment (Supplementary Fig. S10A and 10B). Analysis of the excised tumors using multiplexed and compartment-specific QIF for human TIL subpopulations indicated the presence of human

Published OnlineFirst June 25, 2015; DOI: 10.1158/0008-5472.CAN-14-3510

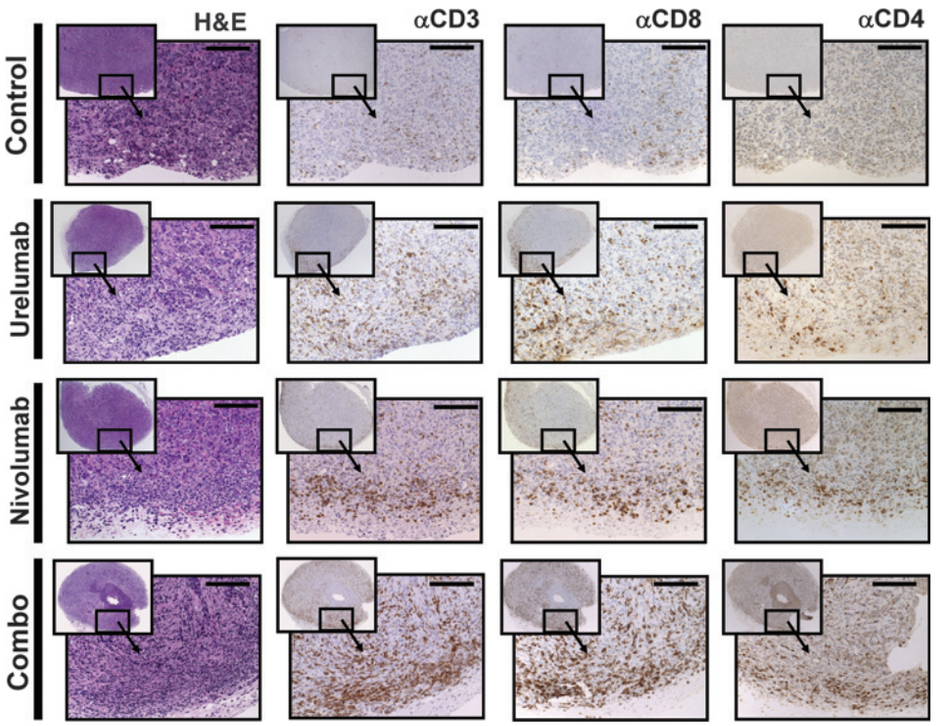

Figure 5.
Increased density of TILs in anti-hCD137 and/or anti-hPD-1 treatment groups. Rag2$^{-/-}$IL2Rγc^{null} mice were treated as described in Fig. 4. On day 22, mice were sacrificed and tumor studied by IHC. Representative histology and IHC images of lymphocyte tumor infiltrate at the invasive margin highlighted by hCD3, hCD4, and hCD8 immunostaining. Microphotographs of tumors subjected to the indicated treatments are presented with two different magnifications (smaller square, ×50; larger square, ×200). Bar, 400 μm.

lymphocytes in the tumor microenvironment (Fig. 7C) and an increase in hCD3$^+$ cells in Combo-treated group in contrast to control group that reached statistical significance only within the tumor compartment ($P < 0.05$; Fig. 7D, left) but not in the stromal compartment (Fig. 7D, right), suggesting more penetration of TILs into the tumor bed. No significant change in the human TIL subpopulations was noted with the other treatment modalities (Fig. 7D). We could not detect CD20$^+$ human B cells in any of the samples analyzed. It is of note, that in tumors from mice treated with combination therapy showed extensive necrosis, a phenomenon not seen in the other treatment groups (data not shown). Moreover, in the urelumab and Combo-treated groups the number of Treg per gram of tumor decreased (Fig. 7E, right) while the CD8$^+$:Treg cells ratio was increased (Fig. 7D, left). In this line, a study at day 22 of human lymphocytes in the peripheral blood from treated mice showed a higher percentage of hCD3$^+$ lymphocytes in the Combo group when compared with the isotype-matched antibody control (hIgG4) group (Supplementary Fig. S10C). Finally, we measured PD-L1/B7-H1 expression using QIF and found positive immunoreaction in both the tumor and stromal compartments (Supplementary Fig. S10D), with a tendency to express higher levels of PD-L1 in tumor than in stromal compartment, particularly in groups treated with anti-hPD1 alone or in combination with anti-hCD137, a finding compatible with a higher penetration of the TILs in the tumor bed as can be seen in Fig. 7C (Combo group).

These results confirm the antitumor activity of the mAbs observed in previous experiments and provide indications of a more pronounced effect with the combination treatment. In addition, the findings open the possibility of studying the mechanisms of action and pharmacodynamics of immunostimulatory antibodies against human targets in an autologous tumor-lymphocyte experimental setting.

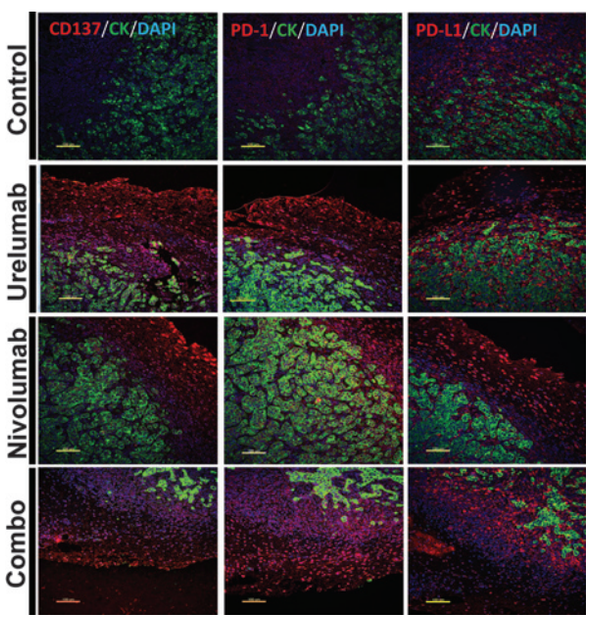

Figure 6.
hCD137, hPD-1, and PD-L1/B7-H1 are expressed in the xenografted tumors. Representative multiplexed immunofluorescence microphotographs showing the protein expression of hCD137 (red fluorescence channel, left), hPD-1 (red channel, middle), and PD-L1 (red channel, right) in the tumor tissues (cytokeratin positive, green channel) from mice subjected to treatment with hIgG4 (control), anti-hCD137 (urelumab), anti-hPD-1 (nivolumab), or the combination (Combo). hCD137 and hPD-1 positivity was distributed predominantly toward the periphery of the tumor surrounding the cytokeratin-positive tumor areas. In contrast, PD-L1 was allocated predominantly toward the tumor center/core, in close association with the tumor nests. Nuclei were stained with DAPI (blue fruorescence channel). Bar, 100 μm.

Published OnlineFirst June 25, 2015; DOI: 10.1158/0008-5472.CAN-14-3510

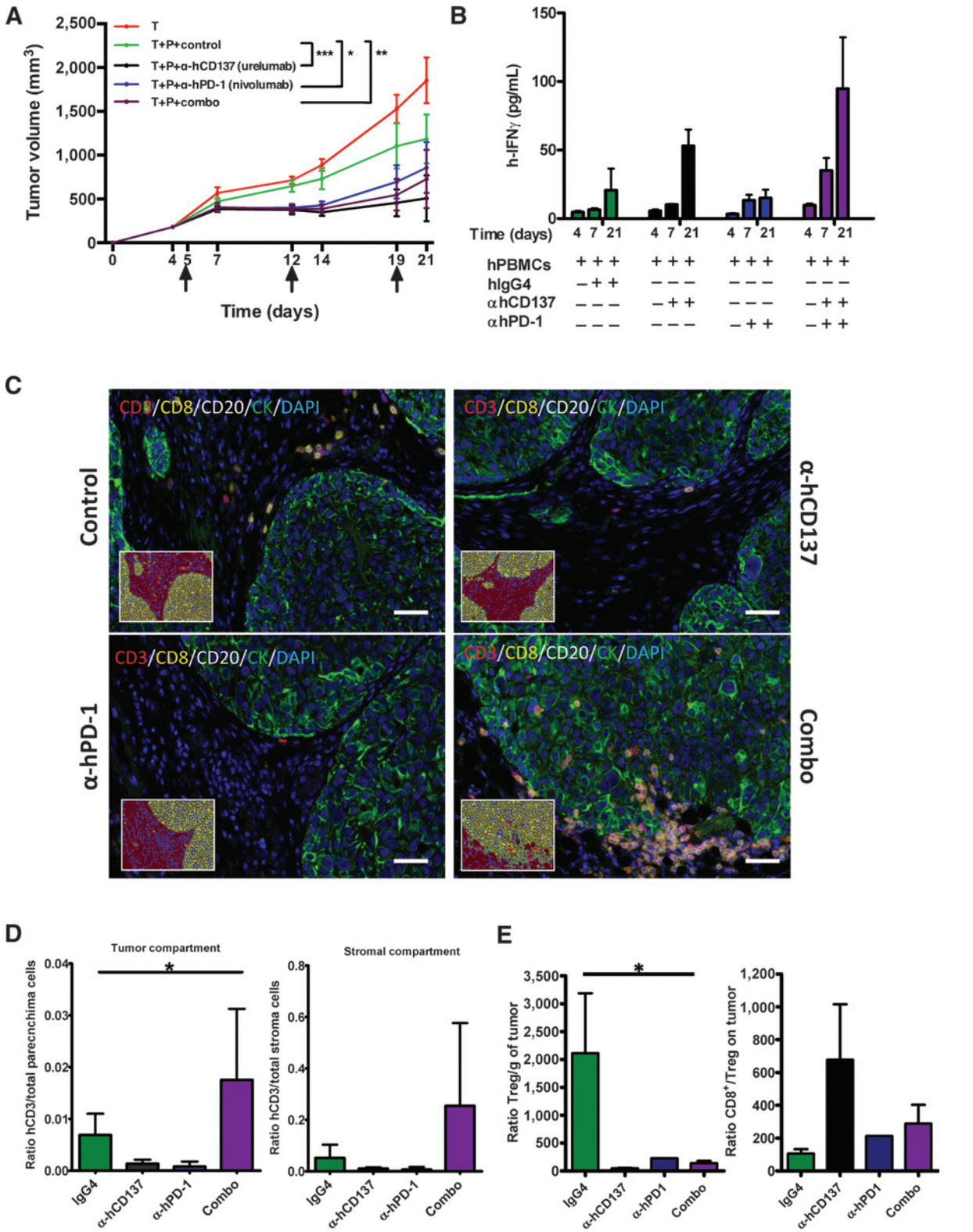

Figure 7.
Anti-hCD137 (urelumab) and anti-hPD-1 (nivolumab) treatment alone or in combination show antitumor effects against a xenografted human gastric cancer transferred with autologous lymphocytes of the patient. Rag2$^{-/-}$IL2Rγ^{null} mice were injected with 7 × 10^6 human PBMCs from a gastric cancer patient on day 0 of the experiment. (*Continued on the following page.*)

Published OnlineFirst June 25, 2015; DOI: 10.1158/0008-5472.CAN-14-3510

Discussion

This study provides a new model to characterize *in vivo* the effects of immunomodulatory mAbs that are being used in the clinic for patients with cancer, an issue that is of particular importance given that predictive modeling in cancer immunotherapy with immunostimulatory mAbs is as yet a largely unmet need.

Transplantable tumors in immunocompetent mice allow for the identification of therapeutic strategies and for detailed analyses of the immune mechanisms of action, but the value of these animal models for predicting the eventual outcome of patients is often questioned (39). There are inherent problems due to major differences in the interplay of artificially inoculated tumor cells and a mouse immune system, which shows major divergences with its human counterpart (40). Oncogene-transgenic mice developing spontaneous tumors might be more predictable for immunotherapies but still rely on a murine immune system and are conceivably less antigenic than those malignancies that have undergone conventional carcinogenesis, with many mutations resulting in neoantigens (41–43). In addition, most immunostimulatory antibodies developed for clinical use do not recognize mouse receptors precluding their preclinical evaluation in these cancer models.

As an alternative, it is conceptually and experimentally possible to repopulate profoundly immunodeficient mice with human lymphocytes in progressively more sophisticated reconstitution models (44). Repopulation can be attained from transferred mature lymphocytes (45) and from $CD34^+$ stem cells that differentiate into lymphocytes in mice (46). Even if caveats exist associated with all these models in the reproduction of human cancer immunotherapy, the models offer interesting insights especially with regard to new therapeutic agents. The only other alternative model for human immunostimulatory mAb in rodents is knockin transgenic mice for the human version of the mAb target molecules. However, these mice also have problems due to the fact that treatments are to be tested in mice bearing tumors of mouse origin and in the context of a murine rather than a human immune system.

For experimentation with clinical-grade anti-hCD137 and anti-hPD-1 mAb, our model of reconstituted $Rag2^{-/-}IL2R\gamma c^{null}$ offers the advantage that the induction of the targeted molecules are expressed on transferred T lymphocytes, in such a way the antibodies can mediate their effects once infused into such mice. The antigen recognition repertoire of human CD4 and CD8 T lymphocytes contains abundant T-cell receptors that mediate recognition of mouse histocompatibility xenoantigens and this is most likely the reason justifying bright and homogeneous surface expression of hPD-1 and hCD137 as a result of activation (45).

The effects of anti-hPD-1 mAb are mainly dependent on the blockade of PD-1 with its natural ligands (PD-L1/B7-H1, PD-L2). Of note, mouse PD-L1/B7-H1 interacts with human PD-1 (47) and human activated T cells express human PD-1. Moreover, if mice are also inoculated with human tumor cells, the malignant cells are induced to express PD-L1/B7-H1 colocalizing for the most extent with T-cell infiltrates (Supplementary Fig. S6). This phenomenon originally described by Dong and colleagues (48) as a mechanism of inducible resistance has been recently observed in cancer patients (5). In contrast, CD137 is a T-cell costimulatory receptor and the effect of anti-hCD137 mAb to increase T-cell function is independent on the presence of CD137-ligand in the system.

One limitation of our model is that the animals develop and most often succumb to xGVHD and as a result experiments must be performed before disease onset, limiting the suitable time span for the experiments to 3 to 4 weeks after engraftment. It is of much interest that this disease is exacerbated by the immunostimulatory mAbs in a $CD4^+$-T cell–dependent manner. Indeed, treatment led to earlier and more severe infiltration of lymphocytes in xGVHD target organs when mice are treated with the clinical-grade immunostimulatory mAbs and this effect is abrogated when $CD4^+$-T cells are depleted from the leukocyte infusion. Experiments reporting on the immunopathologic effects of immunomodulatory mAb in humanized mice have been previously reported by Vudattu and colleagues (49) in humanized mice reconstituted with human $CD34^+$ stem cells and treated with clinical-grade anti-CTLA-4 mAb (ipilimumab). This setting offers possibilities to study treatment strategies for the immune-related adverse events secondary to these new therapeutic agents (50). In particular, liver inflammation selectively observed in mice treated with anti-hCD137 (urelumab) might serve as a model to address the liver inflammation observed in a fraction of cancer patients treated with the anti-hCD137 mAb (22). If controlled T-cell donors are repeatedly used, the model is potentially suitable for correlating individual variability due to gene polymorphisms and with the severity of the adverse reactions and the therapeutic effects.

In our studies we used T cells from donors unrelated to the patient from whom the HT-29 tumor cell line was derived. Under these conditions, there is ample alloreactivity based on the recognition of MHC alloantigens in the transplanted tumor cells. Even though this setting is clearly not mimicking the response against tumor-associated neoantigens, the model permits pharmacodynamic assessments on the effects of immunostimulatory mAbs, such as increases in plasma hIFNγ levels or increases in tumor tissue hCD8:hTreg ratios, thereby offering mechanistic clues to be molecularly explored in the model. In line with this, our results provide evidence for more

(*Continued.*) Explants (7 mm × 7 mm) from the tumor of the same patient were implanted s.c. into the flank of $Rag2^{-/-}IL2R\gamma^{null}$ mice on day 3 of the experiment. Mice ($n = 6$ per group) were treated i.v with anti-hCD137 (urelumab), anti-hPD-1 (nivolumab), combination (nivolumab + urelumab), or isotype control (human IgG4). Tumor volumes were measured twice per week. A, results depict mean ± SEM of tumor growth curves. Arrows, time of treatment administration. T, tumor; P, hPBMCs. B, human IFNγ plasma levels were studied previous to the first mAb dose, after the first and third dose. C, representative multiplexed immunofluorescence microphotographs showing the architecture of tumor xenografts (cytokeratin-positive, green channel) and the presence of TIL subsets (hCD3, red; hCD8, yellow; hCD20 white) from mice treated with hIgG4 (control), anti-hCD137 (urelumab), anti-hPD-1 (nivolumab), or the combination (Combo). Nuclei were stained with DAPI (blue fluorescence). Insets, image segmentation defining tumor (yellow) and stromal compartments (red) as well as the automated cell phenotyping based on multispectral fluorescence analysis. Bar, 100 μm. D, hCD3 T cells/total number cells ratio in tumor (left) and the stroma compartment (right). E, tumor TILs from each treatment group were studied by flow cytometry and results of number of human Tregs per gram of tumor (left) and ratio of human CD8 T cells and human $CD4^+$ $CD25^+$ $FOXP\text{-}3^+$ Tregs (right) are depicted. *, $P < 0.05$; **, $P < 0.01$; ***, $P < 0.001$.

Published OnlineFirst June 25, 2015; DOI: 10.1158/0008-5472.CAN-14-3510

efficacious immune responses and more dense and active tumor infiltrating lymphocytes upon treatment with mAbs that control tumor progression. Similar observations were recently reported in melanomas from patients treated with the anti-PD-1 mAb pembrolizumab (51) and diverse carcinomas treated with the anti-PD-L1 antibody MPDL3280a (52).

Interestingly, T lymphocytes that had trafficked to the tumor preserved the expression of hPD-1 and hCD137 and therefore could be continuously released from PD-1 inhibition while receiving CD137 artificial costimulation. Detailed analyses of such TILs retrieved from excised tumors were possible. Surprisingly, lymphocytes were mainly distributed at the margin of the tumor as has been described in tumor samples from colon cancer patients (53, 54). Such a pattern suggests a common mechanism in tumors hindering lymphocyte invasion of the tumor core. Of note, expression of PD-L1/B7-H1 has been detected mainly at the border of the tumor probably acting as a molecular shield against neighboring T lymphocytes, which perhaps would otherwise actively penetrate the tumor core. Indeed, research in colon cancer has pioneered the important predictive role of the dynamics of activation and location of TILs in the tumor for the progression of the patients (54, 55).

Previous studies in mice have indicated that anti-CD137 and PD-1/PD-L1 blockade is synergistic for tumor treatment (56, 57). In our hands, both antibodies as single agents control allogeneic tumors but the result of combining both mAb is not constantly better. However, TILs in the combined treatment were more numerous and showed more robust signs of activation, which strongly advocates for testing this combination in cancer patients. These results suggest that there is room for testing different doses and dosing schedules of the immunostimulatory mAbs in order to find therapeutic synergy or reduced side effects.

The potential of the model is best illustrated by a human gastric carcinoma xenografted in immunodeficient mice previously injected with tumor-autologous T cells in which the fate of the tumor xenografts is followed under treatment with nivolumab (anti-hPD-1) and urelumab (anti-hCD137). Evidence for delayed tumor growth is remarkable in treated animals, both in monotherapy or in combination, and speaks of the extraordinary potential of these mAb that are being developed in clinical trials, including the PD-1 and CD137-targeted combinatorial treatment (NCT02253992 and NCT02179918). In our experiments, we found significant increases in CD8:Treg ratio and hCD3/tumor cells in the tumor microenvironment of mice treated with the urelumab+nivolumab combination that were absent in tumors from mice undergoing single-agent treatments. Tumor-immunoavatar mouse models of this kind involving treatment with immunostimulatory mAbs may provide useful answers for the design and execution of clinical trials with these novel and promising agents, either in monotherapy or in combination.

Disclosure of Potential Conflicts of Interest

A.J. Korman and M. Jure-Kunkel have ownership interest (including patents) in Bristol-Myers Squibb. I. Melero reports receiving a commercial research grant from Pfizer and Bristol-Myers Squibb, and is a consultant/advisory board member of Bristol-Myers Squibb, Roche, and AstraZeneca. No potential conflicts of interest were disclosed by the other authors.

Authors' Contributions

Conception and design: M.F. Sanmamed, I. Rodriguez, I. Melero
Development of methodology: M.F. Sanmamed, I. Rodriguez, K.A. Schalper, A. Morales-Kastresana, S. Labiano, J.L. Pérez-Gracia, C. Alfaro, G. Mazzolini, F. Sarno, I. Melero
Acquisition of data (provided animals, acquired and managed patients, provided facilities, etc.): M.F. Sanmamed, K.A. Schalper, M.E. Rodriguez-Ruiz, S. Martín-Algarra, F. Sarno
Analysis and interpretation of data (e.g., statistical analysis, biostatistics, computational analysis): M.F. Sanmamed, I. Rodriguez, K.A. Schalper, A. Azpilikueta, M.E. Rodriguez-Ruiz, A. Morales-Kastresana, J.L. Pérez-Gracia, G. Mazzolini, M. Jure-Kunkel, I. Melero
Writing, review, and/or revision of the manuscript: M.F. Sanmamed, I. Rodriguez, K.A. Schalper, M.E. Rodriguez-Ruiz, A. Morales-Kastresana, J.L. Pérez-Gracia, S. Martín-Algarra, M. Hidalgo, M. Jure-Kunkel, I. Melero
Administrative, technical, or material support (i.e., reporting or organizing data, constructing databases): M.F. Sanmamed, A. Azpilikueta, M.E. Rodriguez-Ruiz, S. Labiano, J.L. Pérez-Gracia, C. Alfaro, M. Hidalgo
Study supervision: M.F. Sanmamed, I. Melero
Other (provided reagents and advice on use): A.J. Korman

Acknowledgments

The authors thank Dr. Lieping Chen (University of Yale) for helpful discussions and key reagents; Drs. Sandra Hervas-Stubbs and Diego Alignani for providing technical advice in flow cytometry studies; and Dr. Paul Miller for editing of the article.

Grant Support

This study was supported by MICINN (SAF2008-03294, SAF2011-22831 to I. Melero). I. Melero was also funded by the Departamento de Educación del Gobierno de Navarra and Departamento de Salud del Gobierno de Navarra, Redes temáticas de investigación cooperativa RETIC (RD06/0020/0065) and RTICC, European commission VII framework program (projects ENCITE and IACT) and Fundación Caja Navarra. M.F. Sanmamed is a recipient from a Rio Hortega contract. C. Alfaro was funded by Fundación Mutua Madrileña and receives a Sara Borrell contract from ISCIII. CIBEREHD is funded by Instituto de Salud Carlos III.

The costs of publication of this article were defrayed in part by the payment of page charges. This article must therefore be hereby marked *advertisement* in accordance with 18 U.S.C. Section 1734 solely to indicate this fact.

Received November 28, 2014; revised May 24, 2015; accepted May 31, 2015; published OnlineFirst June 25, 2015.

References

1. Melero I, Hervas-Stubbs S, Glennie M, Pardoll DM, Chen L. Immunostimulatory monoclonal antibodies for cancer therapy. Nat Rev Cancer 2007;7:95–106.
2. Perez-Gracia JL, Labiano S, Rodriguez-Ruiz ME, Sanmamed MF, Melero I. Orchestrating immune check-point blockade for cancer immunotherapy in combinations. Curr Opin Immunol 2014;27C:89–97.
3. Leach DR, Krummel MF, Allison JP. Enhancement of antitumor immunity by CTLA-4 blockade. Science 1996;271:1734–6.
4. Melero I, Shuford WW, Newby SA, Aruffo A, Ledbetter JA, Hellström KE, et al. Monoclonal antibodies against the 4-1BB T-cell activation molecule eradicate established tumors. Nat Med 1997;3:682–5.
5. Pardoll DM. The blockade of immune checkpoints in cancer immunotherapy. Nat Rev Cancer 2012;12:252–64.
6. Melero I, Grimaldi AM, Perez-Gracia JL, Ascierto PA. Clinical development of immunostimulatory monoclonal antibodies and opportunities for combination. Clin Cancer Res 2013;19:997–1008.

7. Song D-G, Ye Q, Poussin M, Harms GM, Figini M, Powell DJ. CD27 costimulation augments the survival and antitumor activity of redirected human T cells *in vivo*. Blood 2012;119:696–706.
8. Ribas A, Kefford R, Marshall MA, Punt CJA, Haanen JB, Marmol M, et al. Phase III randomized clinical trial comparing tremelimumab with standard-of-care chemotherapy in patients with advanced melanoma. J Clin Oncol 2013;31:616–22.
9. Hodi FS, O'Day SJ, McDermott DF, Weber RW, Sosman JA, Haanen JB, et al. Improved survival with ipilimumab in patients with metastatic melanoma. N Engl J Med 2010;363:711–23.
10. Robert C, Thomas L, Bondarenko I, O'Day S, M D JW, Garbe C, et al. Ipilimumab plus dacarbazine for previously untreated metastatic melanoma. N Engl J Med 2011;364:2517–26.
11. Weber JS, Kähler KC, Hauschild A. Management of immune-related adverse events and kinetics of response with ipilimumab. J Clin Oncol 2012;30:2691–7.
12. Topalian SL, Hodi FS, Brahmer JR, Gettinger SN, Smith DC, McDermott DF, et al. Safety, activity, and immune correlates of anti-PD-1 antibody in cancer. N Engl J Med 2012;366:2443–54.
13. Brahmer JR, Tykodi SS, Chow LQM, Hwu W-J, Topalian SL, Hwu P, et al. Safety and activity of anti-PD-L1 antibody in patients with advanced cancer. N Engl J Med 2012;366:2455–65.
14. Hamid O, Robert C, Daud A, Hodi FS, Hwu W-J, Kefford R, et al. Safety and tumor responses with lambrolizumab (anti-PD-1) in melanoma. N Engl J Med 2013;369:134–44.
15. Garon EB, Rizvi NA, Hui R, Leighl N, Balmanoukian AS, Eder JP, et al. Pembrolizumab for the treatment of non–small-cell lung cancer. N Engl J Med 2015;372:2018–28.
16. Powles T, Eder JP, Fine GD, Braiteh FS, Loriot Y, Cruz C, et al. MPDL3280A (anti-PD-L1) treatment leads to clinical activity in metastatic bladder cancer. Nature 2014;515:558–62.
17. Ansell SM, Lesokhin AM, Borrello I, Halwani A, Scott EC, Gutierrez M, et al. PD-1 blockade with nivolumab in relapsed or refractory Hodgkin's Lymphoma. N Engl J Med 2014;372:311–9.
18. Topalian SL, Sznol M, McDermott DF, Kluger HM, Carvajal RD, Sharfman WH, et al. Survival, durable tumor remission, and long-term safety in patients with advanced melanoma receiving nivolumab. J Clin Oncol 2014;32:1020–30.
19. Sznol M, Chen L. Antagonist antibodies to PD-1 and B7-H1 (PD-L1) in the treatment of advanced human cancer–response. Clin Cancer Res 2013;19:5542.
20. Wolchok JD, Kluger H, Callahan MK, Postow MA, Rizvi NA, Lesokhin AM, et al. Nivolumab plus ipilimumab in advanced melanoma. N Engl J Med 2013;369:122–33.
21. Postow MA, Chesney J, Pavlick AC, Robert C, Grossmann K, McDermott D, et al. Nivolumab and Ipilimumab versus Ipilimumab in Untreated Melanoma. N Engl J Med 2015;372:2006–17.
22. Ascierto PA, Simeone E, Sznol M, Fu Y-X, Melero I. Clinical experiences with anti-CD137 and anti-PD1 therapeutic antibodies. Semin Oncol 2010;37:508–16.
23. Kohrt HE, Houot R, Goldstein MJ, Weiskopf K, Alizadeh AA, Brody J, et al. CD137 stimulation enhances the antilymphoma activity of anti-CD20 antibodies. Blood 2011;117:2423–32.
24. Kohrt HE, Houot R, Weiskopf K, Goldstein MJ, Scheeren F, Czerwinski D, et al. Stimulation of natural killer cells with a CD137-specific antibody enhances trastuzumab efficacy in xenotransplant models of breast cancer. J Clin Invest 2012;122:1066–75.
25. Kohrt HE, Colevas AD, Houot R, Weiskopf K, Goldstein MJ, Lund P, et al. Targeting CD137 enhances the efficacy of cetuximab. J Clin Invest 2014;124:2668–82.
26. King MA, Covassin L, Brehm MA, Racki W, Pearson T, Leif J, et al. Human peripheral blood leucocyte non-obese diabetic-severe combined immunodeficiency interleukin-2 receptor gamma chain gene mouse model of xenogeneic graft-versus-host-like disease and the role of host major histocompatibility complex. Clin Exp Immunol 2009;157:104–18.
27. Nervi B, Rettig MP, Ritchey JK, Wang HL, Bauer G, Walker J, et al. Factors affecting human T cell engraftment, trafficking, and associated xenogeneic graft-vs-host disease in NOD/SCID beta2mnull mice. Exp Hematol 2007;35:1823–38.
28. Amarnath S, Mangus CW, Wang JCM, Wei F, He A, Kapoor V, et al. The PDL1-PD1 axis converts human TH1 cells into regulatory T cells. Sci Transl Med 2011;3:111–20.
29. Carroll RG, Carpenito C, Shan X, Danet-Desnoyers G, Liu R, Jiang S, et al. Distinct effects of IL-18 on the engraftment and function of human effector CD8 T cells and regulatory T cells. PLoS ONE 2008;3:e3289.
30. Sagoo P, Ali N, Garg G, Nestle FO, Lechler RI, Lombardi G. Human regulatory T cells with alloantigen specificity are more potent inhibitors of alloimmune skin graft damage than polyclonal regulatory T cells. Sci Transl Med 2011;3:83ra42.
31. Mutis T, van Rijn RS, Simonetti ER, Aarts-Riemens T, Emmelot ME, van Bloois L, et al. Human regulatory T cells control xenogeneic graft-versus-host disease induced by autologous T cells in RAG2$^{-/-}$gammac$^{-/-}$ immunodeficient mice. Clin Cancer Res 2006;12:5520–5.
32. Garralda E, Paz K, López-Casas PP, Jones S, Katz A, Kann LM, et al. Integrated next-generation sequencing and avatar mouse models for personalized cancer treatment. Clin Cancer Res 2014;20:2476–84.
33. Velcheti V, Schalper KA, Carvajal DE, Anagnostou VK, Syrigos KN, Sznol M, et al. Programmed death ligand-1 expression in non-small cell lung cancer. Lab Invest 2014;94:107–16.
34. Schalper KA, Brown J, Carvajal-Hausdorf D, McLaughlin J, Velcheti V, Syrigos KN, et al. Objective measurement and clinical significance of TILs in non-small cell lung cancer. J Natl Cancer Inst 2015;107.
35. Martinez-Forero I, Azpilikueta A, Bolaños-Mateo E, Nistal-Villan E, Palazon A, Teijeira A, et al. T cell costimulation with anti-CD137 monoclonal antibodies is mediated by K63-polyubiquitin-dependent signals from endosomes. J Immunol 2013;190:6694–706.
36. Alfaro C, Suárez N, Martínez-Forero I. Carcinoma-derived interleukin-8 disorients dendritic cell migration without impairing T-cell stimulation. PLoS ONE 2011;6:e17922.
37. Nishikawa H, Sakaguchi S. Regulatory T cells in tumor immunity. Int J Cancer 2010;127:759–67.
38. Zou W, Chen L. Inhibitory B7-family molecules in the tumour microenvironment. Nat Rev Immunol 2008;8:467–77.
39. Ellis LM, Fidler IJ. Finding the tumor copycat. Therapy fails, patients don't. Nat Med 2010;16:974–5.
40. Mestas J, Hughes CCW. Of mice and not men: differences between mouse and human immunology. J Immunol 2004;172:2731–8.
41. Matsushita H, Vesely MD, Koboldt DC, Rickert CG, Uppaluri R, Magrini VJ, et al. Cancer exome analysis reveals a T-cell-dependent mechanism of cancer immunoediting. Nature 2012;482:400–4.
42. DuPage M, Mazumdar C, Schmidt LM, Cheung AF, Jacks T. Expression of tumour-specific antigens underlies cancer immunoediting. Nature 2012;482:405–9.
43. Morales-Kastresana A, Sanmamed MF, Rodriguez I, Palazon A, Martinez-Forero I, Labiano S, et al. Combined immunostimulatory monoclonal antibodies extend survival in an aggressive transgenic hepatocellular carcinoma mouse model. Clin Cancer Res 2013;19:6151–62.
44. Garcia S, Freitas AA. Humanized mice: current states and perspectives. Immunol Lett 2012;146:1–7.
45. Garcia S, Dadaglio G, Gougeon ML. Limits of the human-PBL-SCID mice model: severe restriction of the V beta T-cell repertoire of engrafted human T cells. Blood 1997;89:329–36.
46. Manz MG, Di Santo JP. Renaissance for mouse models of human hematopoiesis and immunobiology. Nat Immunol 2009;10:1039–42.
47. Cheng X, Veverka V, Radhakrishnan A, Waters LC, Muskett FW, Morgan SH, et al. Structure and interactions of the human programmed cell death 1 receptor. J Biol Chem 2013;288:11771–85.
48. Dong H, Strome SE, Salomao DR, Tamura H, Hirano F, Flies DB, et al. Tumor-associated B7-H1 promotes T-cell apoptosis: a potential mechanism of immune evasion. Nat Med 2002;8:793–800.
49. Vudattu NK, Waldron-Lynch F, Truman LA, Deng S, Preston-Hurlburt P, Torres R, et al. Humanized mice as a model for aberrant responses in human T cell immunotherapy. J Immunol 2014;193:587–96.
50. Gangadhar TC, Vonderheide RH. Mitigating the toxic effects of anticancer immunotherapy. Nat Rev Clin Oncol 2014;11:91–9.
51. Tumeh PC, Harview CL, Yearley JH, Shintaku IP, Taylor EJM, Robert L, et al. PD-1 blockade induces responses by inhibiting adaptive immune resistance. Nature 2014;515:568–71.

Published OnlineFirst June 25, 2015; DOI: 10.1158/0008-5472.CAN-14-3510

52. Herbst RS, Soria J-C, Kowanetz M, Fine GD, Hamid O, Gordon MS, et al. Predictive correlates of response to the anti-PD-L1 antibody MPDL3280A in cancer patients. Nature 2014;515:563–7.
53. Fridman WH, Pagès F, Sautès-Fridman C, Galon J. The immune contexture in human tumours: impact on clinical outcome. Nat Rev Cancer 2012;12:298–306.
54. Galon J, Costes A, Sanchez-Cabo F, Kirilovsky A, Mlecnik B, Lagorce-Pagès C, et al. Type, density, and location of immune cells within human colorectal tumors predict clinical outcome. Science 2006;313:1960–4.
55. Fridman WH, Galon J, Pagès F, Tartour E, Sautès-Fridman C, Kroemer G. Prognostic and predictive impact of intra- and peritumoral immune infiltrates. Cancer Res 2011;71:5601–5.
56. Palazón A, Martínez-Forero I, Teijeira A, Morales-Kastresana A, Alfaro C, Sanmamed MF, et al. The HIF-1α hypoxia response in tumor-infiltrating T lymphocytes induces functional CD137 (4-1BB) for immunotherapy. Cancer Discov 2012;2:608–23.
57. Wei H, Zhao L, Li W, Fan K, Qian W, Hou S, et al. Combinatorial PD-1 blockade and CD137 activation has therapeutic efficacy in murine cancer models and synergizes with cisplatin. PLoS ONE 2013;8:e84927.

Published OnlineFirst June 25, 2015; DOI: 10.1158/0008-5472.CAN-14-3510

Cancer Research
The Journal of Cancer Research (1916–1930) | The American Journal of Cancer (1931–1940)

AACR American Association for Cancer Research

Nivolumab and Urelumab Enhance Antitumor Activity of Human T Lymphocytes Engrafted in Rag2$^{-/-}$IL2Rγ^{null} Immunodeficient Mice

Miguel F. Sanmamed, Inmaculada Rodriguez, Kurt A. Schalper, et al.

Cancer Res 2015;75:3466-3478. Published OnlineFirst June 25, 2015.